

2005

Cubic Spline Regression for the Open-Circuit Potential Curves of a Lithium-Ion Battery

Qingzhi Guo

University of South Carolina - Columbia

Ralph E. White

University of South Carolina - Columbia, white@cec.sc.edu

Follow this and additional works at: https://scholarcommons.sc.edu/eche_facpub



Part of the [Chemical Engineering Commons](#)

Publication Info

Published in *Journal of the Electrochemical Society*, Volume 152, Issue 2, 2005, pages A343-A350.

© The Electrochemical Society, Inc. 2005. All rights reserved. Except as provided under U.S. copyright law, this work may not be reproduced, resold, distributed, or modified without the express permission of The Electrochemical Society (ECS). The archival version of this work was published in

Guo, Q. & White, R.E. (2005). Cubic Spline Regression for the Open-Circuit Potential of a Lithium-Ion Battery. *Journal of the Electrochemical Society*, 152(2): A343-A350.

Publisher's Version: <http://dx.doi.org/10.1149/1.1845336>



Cubic Spline Regression for the Open-Circuit Potential Curves of a Lithium-Ion Battery

Qingzhi Guo* and Ralph E. White**^z

Center for Electrochemical Engineering, Department of Chemical Engineering, University of South Carolina, Columbia, South Carolina 29208, USA

A cubic spline regression model was used to fit the experimental open-circuit potential (OCP) curves of two intercalation electrodes of a lithium-ion battery. All the details of an OCP curve were accurately predicted by the resulting model. The number of regression intervals used to fit an OCP curve was determined in a way such that in each regression interval the OCP exhibits a profile predictable by a third-order polynomial. The locations of the data points used to separate regression intervals were optimized. Compared to a polynomial model with the same number of fitting parameters, the cubic spline regression model is more accurate. The cubic spline regression model presented here can be used conveniently to fit complicated profiles such as the OCP curves of lithium-ion battery electrodes.

© 2004 The Electrochemical Society. [DOI: 10.1149/1.1845336] All rights reserved.

Manuscript received July 7, 2004. Available electronically December 30, 2004.

The dependence of the open-circuit potential (OCP) of an intercalation electrode in a lithium-ion battery on the lithium concentration of that electrode usually cannot be explained by a general Nernst equation. Because of this, the equations used in the literature to fit the experimental OCP curve (the dependence of the OCP on the concentration of lithium in the solid phase) of an intercalation electrode vary wildly. For instance, Doyle *et al.*¹ used an equation having two exponential terms and a constant term to fit the experimental OCP curve of a petroleum coke carbon electrode, Ramadass *et al.*² used a rational expression to fit the experimental OCP curve of the carbon electrode of a Sony 18650 cell, and Verbrugge and Koch³ used a modified Nernst equation to fit the experimental OCP curve of a single-fiber carbon electrode. Among those equations, the first two are empirical in nature, and the last one is physically meaningful but can only be used for a few intercalation electrodes having a well-ordered material structure. If the experimental OCP curve of an intercalation electrode exhibits some voltage plateaus corresponding to different staging processes, which is the case for most intercalation electrodes,^{1,4-10} the equations found in the literature are not as accurate as desired.

The Butler-Volmer equation (see Eq. 3 of Ref. 2) used to predict the rate of the electrochemical reaction at an electrode in a lithium-ion battery depends exponentially on the difference between the working potential (the potential difference between the solid phase and solution phase) and the OCP of the electrode. If one is interested in estimating the rate constant of the Butler-Volmer equation from a voltage vs. time discharge curve, any small inaccuracy in knowing the electrode OCP may cause significant error in the estimated value of the rate constant. Therefore, fitting accurately the OCP curve of an intercalation electrode is important to us. On the experimental OCP curve of a carbon electrode with a graphite structure, there are some closely spaced voltage plateaus near 0.1 V (vs. Li metal), and each voltage plateau corresponds to a particular range of lithium intercalation in that electrode.⁴⁻⁷ If the capacity fade of a carbon electrode occurs continuously with cycling due to the branching of charge current to the solvent reduction side reaction,¹¹ one can expect that the carbon electrode will never reach a structure of LiC₆ (fully charged carbon electrode) in its lifetime, and the voltage plateau corresponding to that structure on a low rate discharge curve of that electrode will become narrower and narrower with cycling. Attributing the capacity fade of a lithium-ion battery to the side reaction on its carbon anode may be justified by such a change in the voltage plateau.

Considering that, in general, the experimental OCP curve of an intercalation electrode has a profile much more complicated than

that predicted by a general Nernst equation, an empirical equation is desired to fit such curves. Unfortunately, most empirical equations available in the open literature for that purpose are highly nonlinear in nature with respect to their fitting parameters.^{1-2,10,11} To predict all the voltage plateaus on an OCP curve, an empirical equation may have to include many nonlinear parameters.^{1-2,10-11} Because of this, providing reasonable initial guesses for all the parameters in such an empirical equation is a challenging mission to guarantee the convergence of nonlinear regression.

In this paper, a cubic spline regression model^{12,13} was used to fit the experimental OCP curves of two intercalation electrodes, a carbon electrode, and a cobalt oxide electrode. The advantage of using the cubic spline regression model to fit a complicated profile is demonstrated and compared to a polynomial fit.

Cubic Spline Regression Model

The concept of the spline originated from the drafting technique of using a thin, flexible strip called a spline to draw smooth curves through a set of points.¹⁴ First, consider spline interpolation.¹⁴ The desire is to connect m experimental data points, (x_1, y_1) , $(x_2, y_2), \dots$, and (x_m, y_m) , by a smooth curve. The curve is divided by those points into $m - 1$ intervals. Assume in each interval the data points can be represented by a third-order polynomial

$$y = a_i + b_i x + c_i x^2 + d_i x^3 \quad [1]$$

where x is the independent variable, y is the dependent variable, and a_i , b_i , c_i , and d_i are parameters for the i th interval. To define $m - 1$ intervals completely, $4 \times (m - 1)$ parameters (a_i , b_i , c_i , and d_i) need to be determined. Therefore, $4 \times (m - 1)$ equations are required. One can specify $2 \times m$ equations by assuming that Eq. 1 is valid for all the data points (each interior data point is used twice). One can specify another $2 \times (m - 2)$ equation by assuming that both the first and the second derivatives of the dependent variable with respect to the independent variable are continuous at each interior data point. One can specify the other two equations by assuming that the second derivative of the dependent variable is zero at two end points, (x_1, y_1) and (x_m, y_m) .¹⁴ Once all the $4 \times (m - 1)$ parameters are determined, one can use Eq. 1 to interpolate any point within an interval. The procedure described is the so-called cubic spline interpolation.¹⁴ Whether one should use a third-order polynomial (cubic spline interpolation) or a second-order polynomial (quadratic spline interpolation) depends on the curvature of the data point trajectory. However, using a higher order polynomial is not commonly done.

Cubic spline interpolation is useful when the number of data points is small. If the number is great and all the data points are closely spaced, unfortunately, spline interpolation is inefficient.

* Electrochemical Society Student Member.

** Electrochemical Society Fellow.

^z E-mail: white@enr.sc.edu

Cubic spline regression is similar to cubic spline interpolation. In cubic spline regression, a third-order polynomial is also used for each interval, and the dependent variable and its first and second derivatives are also continuous at all the knots (*i.e.*, the points chosen to define regression intervals).^{12,13} The difference between cubic spline regression and cubic spline interpolation is that only a small number of knots is used in cubic spline regression based on the curvature change of the data point trajectory. A graphic illustration of using knots to define regression intervals is given later. In a cubic spline regression model, Eq. 1 is replaced by the general equation^{12,13}

$$y = a + bx + cx^2 + dx^3 + \sum_{i=1}^k D_i e_i (x_i - x)^3 \quad [2]$$

where a , b , c , d , and e_i are parameters, x_i is the location of the i th knot, k is the number of knots (k knots define $k + 1$ regression intervals because end data points are not used as knots), and D_i is the dummy (or indicator) variable defined to be one in a particular range of x and to be zero otherwise. Equation 2 is a general equation whose exact form varies from one regression interval to another. The model equation for the first interval usually takes the form

$$y = a + bx + cx^2 + dx^3 \quad [3]$$

when all the D_i 's equal zero in the first interval. The model equation for the second interval takes the form

$$y = a + bx + cx^2 + dx^3 + e_1(x - x_1)^3 \quad [4]$$

when $D_1 = 1$ in the second interval. The model equation for the third interval takes the form

$$y = a + bx + cx^2 + dx^3 + e_1(x - x_1)^3 + e_2(x - x_2)^3 \quad [5]$$

when both D_1 and D_2 equal one. As observed from Eq. 3-5, the model equations used for any two adjacent intervals differ only by one term. The slight difference in model equations for two adjacent intervals is created so that the continuity of the dependent variable y , and the continuities of its first and second derivatives at the knot separating those two intervals are all satisfied automatically (x_1 is the location of the knot separating the first and the second intervals, and x_2 is the location of the knot separating the second and the third intervals).^{12,13} Because of this, the curve predicted by the cubic spline regression model is expected to be very smooth. Even though, in general, the regression intervals can be numbered from the first to the last in an increasing order of the independent variable, x , one may elect to number them in a different way (*i.e.*, the regression intervals are numbered in a decreasing order of x). In any case, the model equations for every two adjacent intervals must differ by only one term.

Once the number of knots and their locations are known (knots can be points other than the available experimental data points), one can use Eq. 2 and linear least-squares regression¹⁵ to obtain estimates of parameters, a , b , c , d , and e_i . In most cases, the experimental data points can be fitted with a desired accuracy when using some knots picked by eye according to the curvature change of the data point trajectory, even though the coordinates of knots used in the regression may not be the ones giving rise to the best fit of the data. The coordinates of knots can be optimized by treating them as additional fitting parameters in a model. In this case, nonlinear least-squares regression is required (Eq. 2 is nonlinear with respect to e_i and x_i). If needed, the number of knots and the coordinates of these knots can both be optimized. The number of knots can be optimized by using several consecutive numbers of knots in the regression and the number leading to the best fit is the optimal one.

Multiple Least-Squares Regression

Because in cubic spline regression the available experimental data points are divided into a number of regression intervals using knots and each resulting interval has a different form of the model equation, using multiple least-squares regression to obtain parameter estimates is required. That is, the sum of squared residuals, Φ , is to be minimized¹⁵

$$\Phi = \sum_{i=1}^{k+1} \sum_{j=1}^{n_i} (y_{ij}^* - y_{ij})^2 \quad [6]$$

where n_i is the number of available data points in the i th interval, k is the number of knots defining $(k + 1)$ intervals, y_{ij}^* is the experimental value of the dependent variable at the j th data point of the i th interval, and y_{ij} is the predicted value of the dependent variable at the j th data point of the i th interval.

In linear regression, minimization of Eq. 6 yields¹⁵

$$\theta^* = \left[\sum_{i=1}^{k+1} (\mathbf{J}_i^T \mathbf{J}_i) \right]^{-1} \sum_{i=1}^{k+1} (\mathbf{J}_i^T \mathbf{Y}_i^*) \quad [7]$$

where θ^* is the vector of estimates of parameters (a , b , c , d , and e_i), \mathbf{Y}_i^* is the vector of the experimental values of the dependent variable of the i th interval, and \mathbf{J}_i^T is the transpose of \mathbf{J}_i , the Jacobian matrix of the i th interval

$$(\mathbf{J}_i)_{kl} = (\partial y / \partial \theta_l)_k \quad [8]$$

where the subscript l is used to represent the l th fitting parameter, θ_l , and the subscript k is used to represent the k th data point in the i th interval. In linear regression, the final estimates of all the parameters are obtained after evaluating Eq. 7 once.

In nonlinear regression, Eq. 7 is replaced by¹⁵

$$\Delta \theta^* = \left[\sum_{i=1}^{k+1} (\mathbf{J}_i^T \mathbf{J}_i) \right]^{-1} [\sum_{i=1}^{k+1} \mathbf{J}_i^T (\mathbf{Y}_i^* - \mathbf{Y}_i)] \quad [9]$$

where $\Delta \theta^*$ is the vector of the incremental values of parameters, and \mathbf{Y}_i is the vector of the predicted values of the dependent variable of the i th interval. In nonlinear regression, the final parameter estimates are obtained via an iterative procedure using Eq. 9 until either each element in $\Delta \theta^*$ has a negligible value, or Φ (calculated by Eq. 6) does not change appreciably from one iteration to another.¹⁵ At the end of an iteration, $\Delta \theta^*$ is added to θ^* to update the parameter values in θ^* .

The 95% confidence interval¹⁵ for parameter θ_i can be constructed using

$$\theta_i^* - t_{1-0.05/2} S_E \mathbf{a}_{ii}^{1/2} \leq \theta_i < \theta_i^* + t_{1-0.05/2} S_E \mathbf{a}_{ii}^{1/2} \quad [10]$$

where θ_i^* is the point estimate of parameter θ_i , $t_{1-0.05/2}$ is a value of Student's t distribution with $n-k-4$ degrees of freedom (the total numbers of data points and fitting parameters are n and $k + 4$, respectively), \mathbf{a}_{ii} is the i th element of the principal diagonal of $[\sum_{i=1}^{k+1} (\mathbf{J}_i^T \mathbf{J}_i)]^{-1}$, and S_E is the standard deviation calculated by

$$S_E = \sqrt{\frac{1}{n - k - 4} \sum_{i=1}^{k+1} \sum_{j=1}^{n_i} (y_{ij}^* - y_{ij})^2} \quad [11]$$

Equation 10 can be used to judge whether or not a parameter is significant in a linear model. If zero is included in Eq. 10 for parameter θ_i , one can conclude that parameter is not significant and can be removed from that model. Using Eq. 10 to judge the significance of a parameter in a linear model is equivalent to performing the so-called t -test.¹⁵ One needs to be careful when using Eq. 10 to judge the significance of a parameter in a nonlinear model. In contrast to a linear model, the confidence interval calculated using Eq.

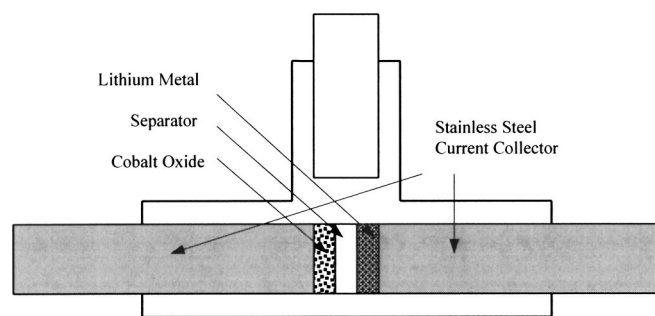


Figure 1. Schematic illustration of a Swagelok-type half-cell used to measure the OCP curves of the cobalt oxide electrode.

10 for a parameter in a nonlinear model is generally bigger than the region where the true value of that parameter may lie. This is due to the so-called correlations between parameters.^{15,16} If a value of zero is not included in any confidence interval obtained using nonlinear regression, it is safe for one to conclude that all the parameters are statistically important. However, if a value of zero is included in a confidence interval, one cannot simply conclude that parameter is statistically insignificant in the nonlinear model.

Experimental

The experimental OCP curves of a cobalt oxide electrode were measured at room temperature (25°C) using a Swagelok-type half-cell setup consisting of a cobalt oxide electrode, a separator, and a lithium foil electrode (see Fig. 1). A Celgard 2400 polypropylene membrane (Charlotte, NC) having a thickness of 25 μm and a porosity of 0.37 was used as the separator. The cobalt oxide electrode used in this work was supplied by the Mine Safety Appliances Company (Sparks, MD). This electrode, which was fabricated using 91% C-022 LiCoO₂, 4% KS-6 graphite, 2% super-P conductive carbon, and 3% polyvinylidene fluoride (PVDF) loaded on one side of a 20 μm thick aluminum foil, has an average thickness of 69.9 μm and an average material loading of 20.1 mg/cm². A 0.38 mm thick lithium metal foil purchased from Aldrich (St. Louis, MO) was used as the counter electrode, which also serves as the reference electrode. The cobalt oxide electrode used in the half-cell was a round disk having a diameter of 1.27 cm, and a theoretical capacity of 3.17×10^{-3} Ah (a value of 0.137 Ah/g was used to calculate the theoretical capacity of the cobalt oxide electrode).¹¹ The half-cell was assembled in an argon-filled glove box. One piece of the cobalt oxide electrode disk, two layers of the separator (each layer has a thickness of 25 μm and a size slightly bigger than an electrode disk), and one piece of the lithium foil disk were used to assemble the half-cell. The LP 30 Selectipur electrolyte purchased from E. Merck (Hawthorne, NY) with a LiPF₆ concentration of 1.0 M in a 1:1 v/v ethylene carbonate-dimethyl carbonate (EC-DMC) solvent was used to fill the cell. After the separator and two electrodes were sufficiently wetted by the electrolyte, the cell was sealed and removed from the glove box. The cell was first cycled several times before any OCP curve was measured. Each cycle consists of a 0.1 C rate constant current charge process, a 4.2 V constant voltage charge process (the cutoff current was 30 μA), and a 0.1 C rate constant current discharge process (the cutoff voltage was 3.75 V). Cycling was performed on the cell in order to stabilize its charge/discharge performance because the solvent reduction reaction is expected to be active during the first few charge/discharge cycles. In this work, the OCP curves of the cobalt oxide electrode were measured after the cell was cycled three times to confirm that the charge and discharge performance of the cell was reproducible. A 16-channel battery test system purchased from Arbin (College Station, TX) was used to cycle the cell and measure its OCP curves. The OCP curve of the cobalt oxide electrode for a charge process was measured by charging the half-cell at a constant current of 30 μA (a rate lower than

1/100 C) to the cutoff voltage of 4.2 V from a fully discharged state (the cell voltage was 3.75 V when discharged at 30 μA), and the OCP curve of the cobalt oxide electrode for a discharge process was measured by discharging at the same current to the cutoff voltage of 3.75 V from a fully charged state (the cell voltage was 4.2 V when charged at 30 μA). Because the charge/discharge current was small during the OCP measurements, the voltage drop across the separator and the polarization voltage loss on both the cathode and the anode were expected to be negligible. Therefore, the OCP of the cobalt oxide electrode was approximated by the voltage of the cell in this work.

The low-rate charge and discharge curves measured by the Mine Safety Appliances Company using a coin cell setup consisting of a carbon electrode, a separator, and a lithium foil electrode were used in this work as the OCP curves of the carbon electrode. The carbon electrode, which was fabricated using 91.5% mesocarbon microbead (MCMB) 2528, 0.5% super P conductive carbon, and 8% PVDF loaded on one side of a copper foil, has an average thickness of 76.2 μm and an average material loading of 9.7 mg/cm². Both the carbon electrode and the lithium foil electrode used in the coin cell were round disks having a diameter of 1.587 cm. The theoretical capacity of the carbon electrode disk was 6.32×10^{-3} Ah (a value of 0.372 Ah/g was used to calculate the theoretical capacity of the carbon electrode). To make the coin cell, one piece of the carbon electrode disk, one layer of 25 μm thick Celgard 2300 polypropylene-polyethylene-polypropylene separator (slightly bigger in size than an electrode disk), and one piece of the lithium foil disk were used. The proprietary electrolyte of the Mine Safety Appliances Company with a LiPF₆ concentration of 1.0 M in a 30:5:35:30 v/v EC-PC-EMC-DEC solvent was used to fill the cell. The coin cell was cycled three times using a 500 μA constant current charge process, a 20 mV constant voltage charge process (the cutoff current was 50 μA), and a 500 μA constant current discharge process (the cutoff voltage was 2.0 V). The charge and discharge curves measured in the third cycle were used as the OCP curves of the carbon electrode for a charge process and for a discharge process, respectively.

In this work, the OCP was first recorded vs. Q_c , the charge capacity in Ah, or vs. Q_d , the discharge capacity in Ah. Then Q_c or Q_d was converted to x , a dimensionless state of charge, by

$$x = \frac{Q_c}{Q_{\text{theoretical}}} \quad \text{or} \quad x = \frac{Q_{d,\text{total}} - Q_d}{Q_{\text{theoretical}}} \quad [12]$$

for the carbon electrode assumed to have a structure of Li_xC₆ or by

$$x = 1 - \frac{Q_c}{2Q_{\text{theoretical}}} \quad \text{or} \quad x = 1 - \frac{Q_{d,\text{total}} - Q_d}{2Q_{\text{theoretical}}} \quad [13]$$

for the cobalt oxide electrode assumed to have a structure of Li_xCoO₂. In Eq. 12 and 13, $Q_{\text{theoretical}}$ stands for the theoretical capacity of the intercalation electrode in ampere-hours, and $Q_{c,\text{total}}$ and $Q_{d,\text{total}}$ stands for the total charge and discharge capacities in ampere-hours, respectively. To obtain Eq. 12 and 13, we assume that the fully discharged cobalt oxide electrode has a dimensionless concentration of 1 and a structure of LiCoO₂, and the fully discharged carbon electrode has a dimensionless concentration of 0 and a structure of C₆.^{1,5,7} When $Q_{c,\text{total}} = Q_{d,\text{total}} = Q_{\text{theoretical}}$, the fully charged carbon electrode has a dimensionless concentration of 1 and a structure of LiC₆, and the fully charged cobalt oxide electrode has a dimensionless concentration of 1 and a structure of Li_{0.5}CoO₂ (in Eq. 13, the value of x ranges from 0.5 to 1).^{1,5,7}

Results and Discussion

In this work, all the experimental OCP curves were fitted by the cubic spline regression model along with the optimization of the coordinates of knots x_i . It is important to note that including x_j in cubic spline regression makes Eq. 2 become nonlinear with respect to its fitting parameters. Therefore, providing reasonable initial

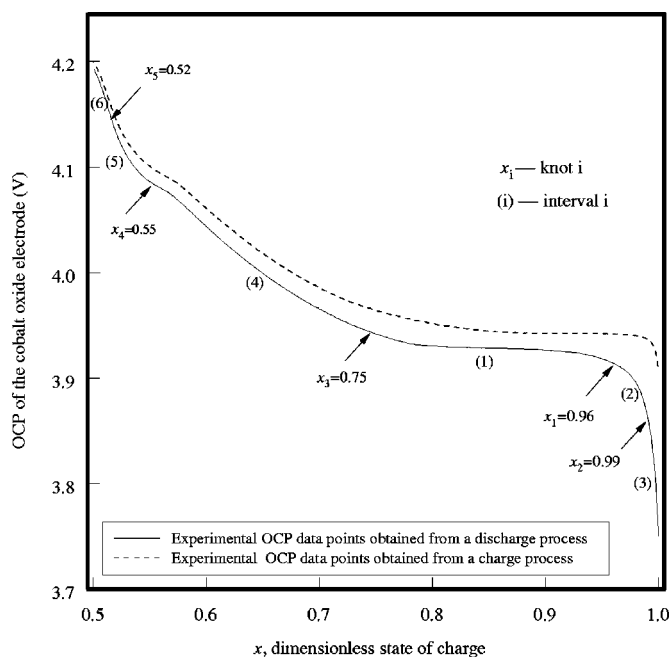


Figure 2. The experimental OCP curves of the cobalt oxide electrode obtained in both a charge process and a discharge process.

guesses for fitting parameters is important to guarantee the convergence of regression. To fit an experimental curve in this work, two or three consecutive numbers were first tried for k and the assumed values (by eye) were used for x_i values in linear regressions (to start with, x_i values were excluded from the fitting parameter list). To obtain the final estimates of a , b , c , d , e_i , and x_i , the number for k leading to a desired accuracy in linear regression and the resulting values of a , b , c , d , e_i , and x_i were then used as initial guesses in nonlinear regression (x_i was added to the fitting parameter list).

The experimental OCP curves of the cobalt oxide electrode obtained from both a discharge process and a charge process are presented in Fig. 2. As observed in Fig. 2, these OCP curves exhibit a hysteresis behavior. That is, the OCP curve measured in a low rate charge process does not agree with that measured in a low rate discharge process. Similar phenomena have already been reported in the literature.¹⁷⁻¹⁹ The charge/discharge current of $30 \mu\text{A}$ used in this work to measure an OCP curve of the cobalt oxide electrode was small (lower than $1/100 \text{ C rate}$) and was not expected to cause any significant loss in the half-cell voltage. Such a low rate current has also been used in the literature to measure the OCP curve of an intercalation electrode.²⁰ In this work, the OCP curve of the cobalt oxide electrode measured in a charge process was fitted separately from that measured in a discharge process. For the experimental OCP curve obtained in a discharge process, five knots were used in the regression, and for the experimental OCP curve obtained in a charge process, four knots were used. Using knots to define regression intervals for the experimental OCP curve obtained in a discharge process are presented in Fig. 2. As observed, six regression intervals are defined by five knots, and each resulting regression interval exhibits a profile predictable by a third-order polynomial. The coordinates of all the knots presented in Fig. 2 are initial guesses used in nonlinear regression.

The OCP curves of the cobalt oxide electrode predicted by the cubic spline regression model are compared with the experimental curves in Fig. 3. As observed, two experimental OCP curves were fitted very well. The goodness of fit is also demonstrated in Fig. 4 from the plot of $y_{ij}^* - y_{ij}$ vs. x , the dimensionless state of charge of the cobalt oxide electrode. As observed in Fig. 4, except for a few scatters, y_{ij} , the predicted OCP deviates from y_{ij}^* , the experimental

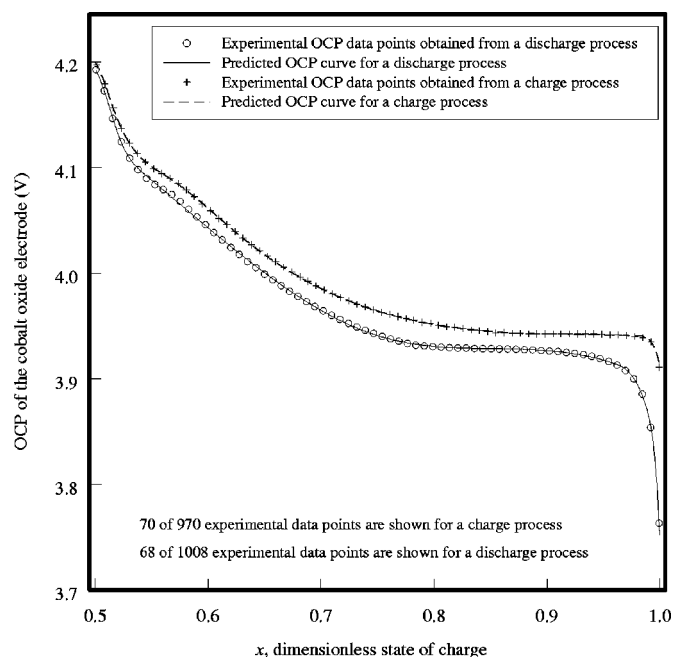


Figure 3. Comparison of the experimental OCP curves of the cobalt oxide electrode and the curves predicted by cubic spline regression. 12-digit numerical precision was used in the regression.

OCP, only by a small value ($\leq 0.003 \text{ V}$) at each data point. Moreover, $y_{ij}^* - y_{ij}$ is randomly distributed around a mean of zero. The dummy variables D_i defined in cubic spline regression are presented in Table I. The exact forms of model equations used in fitting the experimental OCP curve obtained in a discharge process are demonstrated in the Appendix. Table I also presents the 95% confidence intervals for all the fitting parameters. As observed in Table I, a value of zero is not included in any confidence interval. Therefore, all the parameters are statistically significant for the cobalt oxide electrode. The first regression interval was chosen here to be located

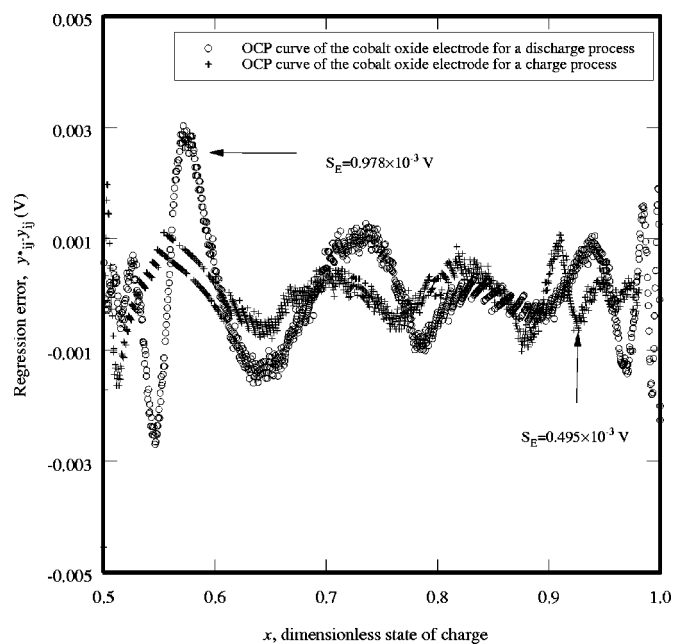


Figure 4. Distribution of the regression error in fitting the experimental OCP curves of the cobalt oxide electrode using cubic spline regression.

Table I. The 95% confidence intervals for all the parameters used in Eq. 2 to fit the OCP curves of the cobalt oxide electrode.

k , the number of knots	Discharge process 5	Charge process 4
x_i , the knot coordinate	$x_1 = 0.95912 \pm 0.00124$ $x_2 = 0.98829 \pm 0.00060$ $x_3 = 0.74787 \pm 0.00318$ $x_4 = 0.54438 \pm 0.00177$ $x_5 = 0.52170 \pm 0.00233$	$x_1 = 0.98167 \pm 0.00060$ $x_2 = 0.63193 \pm 0.00221$ $x_3 = 0.56330 \pm 0.00115$ $x_4 = 0.51672 \pm 0.00117$
First interval	$x_3 < x < x_1$	$x_2 < x \leq x_1$
D_j , the dummy variable	$D_1 = 1$ at $x > x_1$, $D_1 = 0$ at $x \leq x_1$ $D_2 = 1$ at $x > x_2$, $D_2 = 0$ at $x \leq x_2$ $D_3 = 1$ at $x \leq x_3$, $D_3 = 0$ at $x > x_3$ $D_4 = 1$ at $x \leq x_4$, $D_4 = 0$ at $x > x_4$ $D_5 = 1$ at $x \leq x_5$, $D_5 = 0$ at $x > x_5$	$D_1 = 1$ at $x > x_1$, $D_1 = 0$ at $x \leq x_1$ $D_2 = 1$ at $x \leq x_2$, $D_2 = 0$ at $x > x_2$ $D_3 = 1$ at $x \leq x_3$, $D_3 = 0$ at $x > x_3$ $D_4 = 1$ at $x \leq x_4$, $D_4 = 0$ at $x > x_4$
a (V)	$(1.0188 \pm 0.0165) \times 10^1$	6.4653 ± 0.0187
b (V)	$(-2.1993 \pm 0.0593) \times 10^1$	-8.0590 ± 0.0714
c (V)	$(2.5772 \pm 0.0709) \times 10^1$	8.5952 ± 0.0900
d (V)	$(-1.0074 \pm 0.0282) \times 10^1$	-3.0614 ± 0.0374
e_1 (V)	$(-1.1715 \pm 0.1420) \times 10^3$	$(-4.2630 \pm 0.4756) \times 10^3$
e_2 (V)	$(-3.8652 \pm 0.4799) \times 10^4$	$(4.3245 \pm 0.3423) \times 10^1$
e_3 (V)	$(1.6073 \pm 0.0284) \times 10^1$	$(-4.6228 \pm 0.1896) \times 10^2$
e_4 (V)	$(-1.2383 \pm 0.2594) \times 10^3$	$(4.2944 \pm 0.7597) \times 10^3$
e_5 (V)	$(4.5416 \pm 0.7165) \times 10^3$	
S_E , the standard deviation (V)	9.7772×10^{-4}	4.9544×10^{-4}

in the middle region of the data point range rather than at one end. Choosing a middle region as the first regression interval was to avoid round-off error. One may observe from Fig. 2 or 3 that not only is there a steep OCP profile on the rightmost side, but also a fast change in OCP on the leftmost side. If the first regression interval is chosen to be at one end instead, a very negative value of d in Eq. 2 is obtained in order to reflect the fast OCP decay in the first interval. As observed in Fig. 2 or 3, the OCP changes mildly with the dimensionless state of charge x in its middle region. To predict a mild OCP change in an interval, the fast OCP decay predicted by term dx^3 has to be neutralized (dx^3 exists in the model equation for each interval), and very positive values are obtained for many e_i . When low numerical precision is used in the regression, round-off error is significant, because the relatively small but nontrivial difference between two almost equally large terms having different signs is likely rounded off. In contrast, when the first interval is chosen to be in the middle region of x , round-off error can be avoided (neutralizing a large term is not needed) and 12-digit precision is sufficient to guarantee the accuracy of regression.

Recently, Stamps *et al.*²¹ used a 9th-order polynomial to fit the OCP curve of a Sony 18650 lithium-ion battery. A polynomial equation may be more convenient to use than a general spline equation such as Eq. 2, because the exact form of the polynomial does not vary with data points, and there is no need to define knots and intervals in polynomial regression. In this work, the appropriateness of using a polynomial equation to fit an OCP curve of the cobalt oxide electrode was evaluated. The polynomial equation has a form

$$y = \sum_{i=0}^m a_i x^i \quad [14]$$

where m is the order of the polynomial, and a_i is a parameter. Two different values were used for m in Eq. 14, and the OCP curves of the cobalt oxide electrode predicted by polynomial regression for a discharge process are compared with the experimental curve in Fig. 5. As observed in Fig. 5, the 15th-order polynomial can be used to fit the experimental data with a desired accuracy. Unfortunately, the

goodness in fitting the experimental OCP curve by the 15th-order polynomial was achieved at the cost of using 32-digit numerical precision. An attempt to lower the precision to a smaller number, *i.e.*, 16 digits, caused significant error in the regression. We observed that all a_i 's estimated using the 32-digit precision had a magnitude in the order of 10^7 - 10^{12} , and among all the a_i 's, the number of positive signs was almost equal to the number of negative signs.

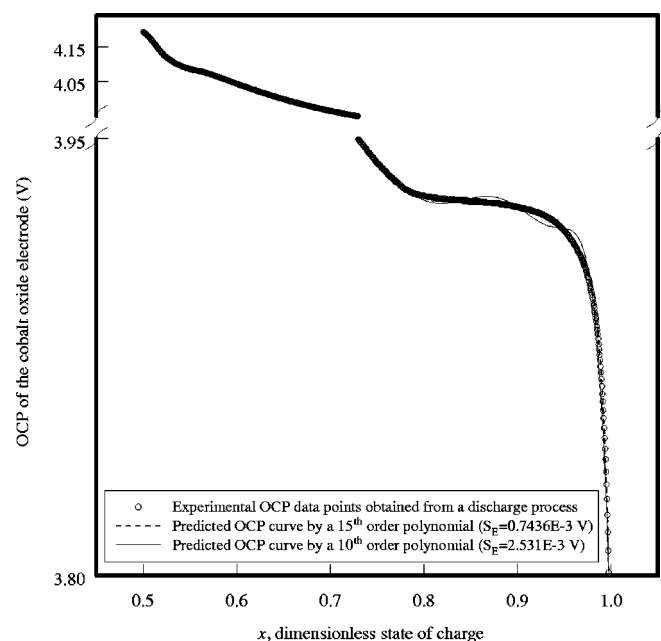


Figure 5. Comparison of the experimental OCP curve of the cobalt oxide electrode for a discharge process and the curves predicted by polynomial regression. Two different orders, $m = 10$ and 15, were used in Eq. 14, and 32-digit precision was used in polynomial regression.

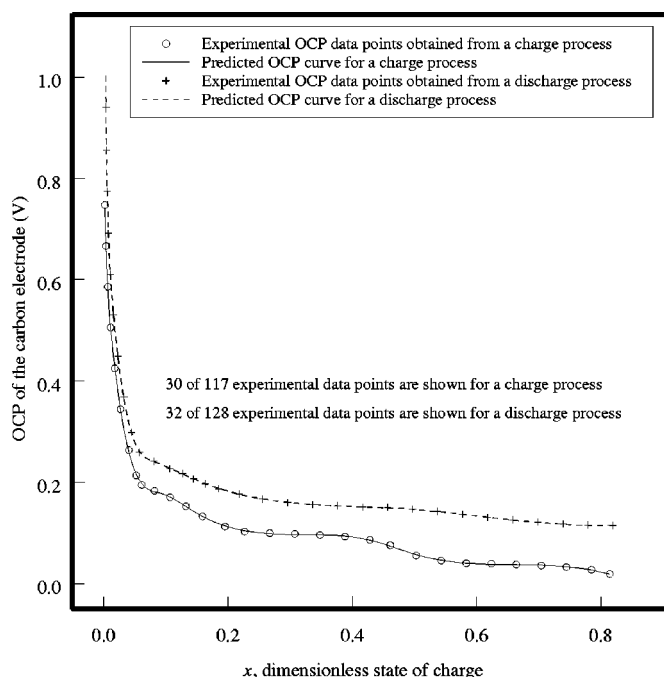


Figure 6. Comparison of the experimental OCP curves of the carbon electrode and the curves predicted by cubic spline regression. 12-digit precision was used in the regression.

One can imagine that round-off error is significant if lower digit precision is used in the regression, because a finite value in the OCP of the cobalt oxide electrode is determined by the relatively small difference between two groups of terms having a large magnitude. In contrast, only 12-digit precision is required in cubic spline regres-

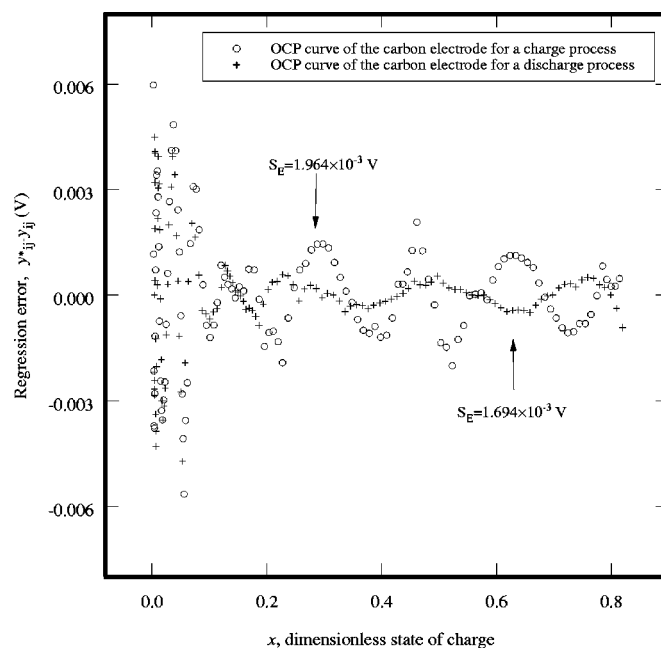


Figure 7. Distribution of the regression error in fitting the experimental OCP curves of the carbon electrode using cubic spline regression.

sion to guarantee the accuracy. Therefore, the cubic spline regression method is numerically more tolerant than the polynomial model.

Figure 6 presents the comparison of the experimental curves of the carbon electrode and its predicted OCP curves by cubic spline regression. As observed in Fig. 6, similar to the cobalt oxide electrode, the experimental OCP curve of the carbon electrode obtained

Table II. The 95% confidence intervals for all the parameters used in Eq. 2 to fit the OCP curve of the carbon electrode. 12-digit precision was used in the regression.

k , the number of knots	Discharge process	Charge process
		5
x_i , the knot coordinate	$x_1 = (4.7423 \pm 0.3329) \times 10^{-1}$ $x_2 = (1.6833 \pm 0.4582) \times 10^{-1}$ $x_3 = (7.8218 \pm 0.2513) \times 10^{-2}$ $x_4 = (1.5397 \pm 0.0512) \times 10^{-2}$ $x_5 = (5.9697 \pm 0.1060) \times 10^{-3}$	^a $x_1 = 5.0000 \times 10^{-1}$ (fixed) $x_2 = (4.3510 \pm 0.1545) \times 10^{-1}$ $x_3 = (1.4804 \pm 0.1857) \times 10^{-1}$ $x_4 = (9.1037 \pm 0.4839) \times 10^{-2}$ $x_5 = (1.3432 \pm 0.0749) \times 10^{-2}$
First interval	$x > x_1$	
D_i , the dummy variable	$D_i = 1$ at $x \leq x_i$, $D_i = 0$ at $x > x_i$ ($i = 1-5$)	
a (V)	^b $(-6.3949 \pm 9.6734) \times 10^{-2}$	1.3313 ± 0.1603
b (V)	1.2623 ± 0.4862	-5.8437 ± 0.7818
c (V)	-2.3261 ± 0.7979	8.8196 ± 1.2502
d (V)	1.2853 ± 0.4282	-4.4493 ± 0.6561
e_1 (V)	-3.7276 ± 0.4261	$(2.9545 \pm 0.7915) \times 10^1$
e_2 (V)	^b $(1.4102 \pm 1.5662) \times 10^1$	$(-3.3124 \pm 0.6804) \times 10^1$
e_3 (V)	$(-1.1094 \pm 0.0668) \times 10^3$	$(9.9138 \pm 7.0447) \times 10^1$
e_4 (V)	$(-1.0475 \pm 0.1351) \times 10^5$	$(-8.2875 \pm 0.5537) \times 10^2$
e_5 (V)	$(-9.4697 \pm 1.3514) \times 10^6$	$(-7.3116 \pm 1.3316) \times 10^4$
S_E , the standard deviation (V)	1.6935×10^{-3}	1.9637×10^{-3}

^a x_1 was fixed to a value in this work due to the difficulty in convergence.

^b If x_i values are fixed to the point estimates presented, the confidence intervals for a and e_2 are $(-6.3949 \pm 3.2232) \times 10^{-2}$ and $(1.4102 \pm 0.2151) \times 10^1$, respectively. The confidence intervals for the other parameters are also made smaller than those presented.

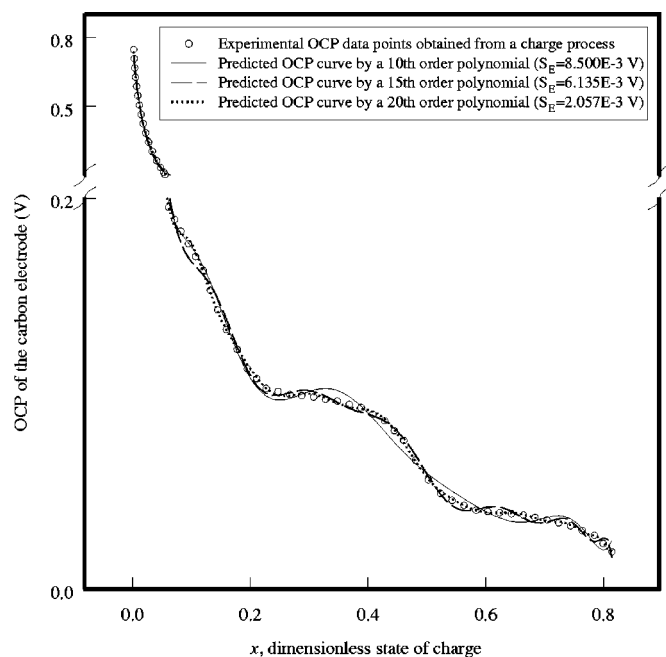


Figure 8. Comparison of the experimental OCP curve of the carbon electrode for a charge process and the curves predicted by polynomial regression. Three different orders, $m = 10, 15,$ and $20,$ were used in Eq. 14, and 32-digit precision was used in polynomial regression.

in a charge process differs from that obtained in a discharge process. These two OCP curves were also fitted separately in this work. One can also observe from Fig. 6 that each experimental curve exhibits three voltage plateaus and a spike. This agrees with the results reported in the literature for a MCMB carbon electrode.⁴⁻⁷ To predict all the details of a curve accurately, five knots were used and six regression intervals were defined in this work. As demonstrated in Fig. 6, all the voltage plateaus are effectively and accurately predicted. The goodness of fit can also be appreciated from the plot of $y_{ij}^* - y_{ij}$ vs. x , the dimensionless state of charge of the carbon electrode, presented in Fig. 7. To fit an experimental OCP curve of the carbon electrode, the regression intervals were numbered from the first to the last in a decreasing order of x . The dummy variables D_i used in the regression are presented in Table II. The 95% confidence intervals for all the fitting parameters are presented in Table II as well. One may observe that a value of zero is included in the confidence intervals for a and e_2 when fitting the experimental OCP curve obtained in a discharge process. This indicates uncertainty in determining the values of these two parameters. However, as mentioned before, we cannot simply conclude that these two parameters are statistically insignificant. In some cases, the uncertainty of a parameter in a nonlinear model can be explained by parameter correlations.¹⁵⁻¹⁶ To confirm this explanation is also valid here, we fixed the values of x_i and calculated the 95% confidence intervals for the remaining parameters, $a, b, c, d,$ and e_i (if x_i 's are not included as fitting parameters, the cubic spline regression model becomes linear and parameter correlations are removed). The newly obtained confidence intervals for a and e_2 are also presented in Table II. As observed, neither new confidence includes a value of zero. This indicates that all the parameters presented in Table II are significant.

In this work, the appropriateness of using a polynomial equation to fit an OCP curve of the carbon electrode was evaluated by using three different numbers for m in Eq. 14. The OCP curves of the carbon electrode predicted by polynomial regression for a charge process are compared with the experimental curve in Fig. 8. One can see from Fig. 8 that the 20th-order polynomial can be used to fit the experimental data with a desired accuracy. Unfortunately, similar to

fitting the experimental OCP curve of the cobalt oxide electrode, the goodness in fitting the OCP curve by the 20th-order polynomial was achieved at the cost of using 32-digit numerical precision, and an attempt to lower the precision to a smaller number, *i.e.*, 16 digits, caused significant error in the regression.

Conclusions

The cubic spline regression model presented here is useful for fitting complicated profiles such as the experimental OCP curves of intercalation electrodes. Even though a few intervals need to be defined and the model equation has a form varying from one interval to another, the model predictions are smooth within the entire range of the experimental data points because the dependent variable, and its first and second derivatives, are all continuous within that range. Round-off error can be avoided in cubic spline regression by choosing the first regression interval away from a steep portion of an OCP curve.

In general, using a high-order polynomial equation to fit an OCP curve of an intercalation electrode is not recommended because such a fit does not provide the accuracy needed.

Acknowledgments

The authors are grateful for the financial support of the project by the National Reconnaissance Office (NRO) under contract no. NRO-000-03-C-0122.

The University of South Carolina assisted in meeting the publication costs of this article.

Appendix

The Discharge Process of the Cobalt Oxide Electrode^a

The exact form of Eq. 2 for the first regression interval, $x_3 < x < x_1$, is

$$y = a + bx + cx^2 + dx^3 \quad [\text{A-1}]$$

The exact form of Eq. 2 for the second regression interval, $x_1 < x < x_2$, is

$$y = a + bx + cx^2 + dx^3 + e_1(x - x_1)^3 \quad [\text{A-2}]$$

The exact form of Eq. 2 for the third regression interval, $x > x_2$, is

$$y = a + bx + cx^2 + dx^3 + e_1(x - x_1)^3 + e_2(x - x_2)^3 \quad [\text{A-3}]$$

The exact form of Eq. 2 for the fourth regression interval, $x_4 < x < x_3$, is

$$y = a + bx + cx^2 + dx^3 + e_3(x - x_3)^3 \quad [\text{A-4}]$$

The exact form of Eq. 2 for the fifth regression interval, $x_5 < x < x_4$, is

$$y = a + bx + cx^2 + dx^3 + e_3(x - x_3)^3 + e_4(x - x_4)^3 \quad [\text{A-5}]$$

The exact form of Eq. 2 for the sixth regression interval, $x \leq x_5$, is

$$y = a + bx + cx^2 + dx^3 + e_3(x - x_3)^3 + e_4(x - x_4)^3 + e_5(x - x_5)^3 \quad [\text{A-6}]$$

List of Symbols

- a fitting parameter (see Eq. 2-5, and A-1 through A-6), V
- a_i fitting parameter (see Eq. 1 and 14), V
- a_{ii} i th element of the diagonal of the matrix $\mathbf{a} = [\sum_{i=1}^{k+1} (\mathbf{J}_i^T \mathbf{J}_i)]^{-1}$
- b fitting parameter (see Eq. 2-5, and A-1 through A-6), V
- b_i fitting parameter (see Eq. 1), V
- c fitting parameter (see Eq. 2-5, and A-1 through A-6), V
- c_i fitting parameter (see Eq. 1), V
- d fitting parameter (see Eq. 2-5, and A-1 through A-6), V
- d_i fitting parameter (see Eq. 1), V
- D_i dummy variable which takes a value of 1 or 0
- e_i fitting parameter (see Eq. 2), V
- \mathbf{J}_i Jacobian matrix of the i th regression interval
- k number of knots
- m order of the polynomial equation, see Eq. 14

^a See Fig. 2.

n	total number of experimental data points
n_i	number of experimental data points in the i th regression interval
OCP	open-circuit potential of an intercalation electrode, V
Q_c	charge capacity of an intercalation electrode, Ah
$Q_{c,\text{total}}$	total charge capacity of an intercalation electrode, Ah
Q_d	discharge capacity of an intercalation electrode, Ah
$Q_{d,\text{total}}$	total discharge capacity of an intercalation electrode, Ah
$Q_{\text{theoretical}}$	theoretical capacity of an intercalation electrode, Ah
S_E	standard deviation, V
$t_{1-0.05/2}$	value of Student's t distribution that depends on $(n-k-4)$, degrees of freedom
x	independent variable (dimensionless state of charge of the intercalation electrode)
x_i	coordinate of the i th knot in the cubic spline regression model
y	dependent variable (the OCP), V
y_{ij}	predicted value of the dependent variable at the j th data point of the i th interval, V
y_{ij}^*	experimental value of the dependent variable at the j th data point of the i th interval, V
\mathbf{Y}_i	vector of the predicted values of the dependent variable of the i th regression interval, V
\mathbf{Y}_i^*	vector of the experimental values of the dependent variable of the i th regression interval, V

Greek

θ	vector of fitting parameters (a, b, c, d, e_1 , and x_i), V
θ_i	i th fitting parameter, V
θ^*	vector of the point estimates of fitting parameters, V
θ_i^*	point estimate of the i th fitting parameter, V
$\Delta\theta^*$	vector of the incremental values of fitting parameters, V
Φ	sum of squared residuals, V^2

Superscripts

T	transpose
-1	inverse

References

1. M. Doyle, J. Newman, A. S. Gozdz, C. N. Schmutz, and J. Tarascon, *J. Electrochem. Soc.*, **143**, 1890 (1996).
2. P. Ramadass, B. Haran, R. White, and B. N. Popov, *J. Power Sources*, **123**, 230 (2003).
3. M. W. Verbrugge and B. J. Koch, *J. Electrochem. Soc.*, **143**, 600 (1996).
4. T. Ohzuku, Y. Iwakoshi, and K. Sawai, *J. Electrochem. Soc.*, **140**, 2490 (1993).
5. Z. Jiang, M. Alamgir, and K. M. Abraham, *J. Electrochem. Soc.*, **142**, 333 (1995).
6. R. Fong, U. V. Sacken, and J. R. Dahn, *J. Electrochem. Soc.*, **137**, 2009 (1990).
7. N. Takami, A. Satah, M. Hara, and T. Ohsaki, *J. Electrochem. Soc.*, **142**, 371 (1995).
8. D. Guyomard and J. M. Tarascon, *J. Electrochem. Soc.*, **139**, 937 (1992).
9. R. Kanno, Y. Kawamoto, Y. Takeda, S. Ohashi, N. Imanishi, and O. Yamamoto, *J. Electrochem. Soc.*, **139**, 3397 (1992).
10. R. Darling and J. Newman, *J. Electrochem. Soc.*, **144**, 4201 (1997).
11. G. Sikha, B. N. Popov, and R. E. White, *J. Electrochem. Soc.*, **151**, A1104 (2004).
12. L. C. Marsh and D. R. Cormier, *Spline Regression Models*, Sage Publications, Thousand Oaks, CA (2001).
13. L. C. Marsh, *SUGI*, **8**, 723 (1983).
14. S. C. Chapra and R. P. Canale, *Numerical Methods for Engineers with Programming and Software Applications*, 3rd ed., WCB/McGraw-Hill, New York (1998).
15. A. Constantinidis and N. Mostoufi, *Numerical Methods for Chemical Engineers with MATLAB Applications*, Prentice-Hall, Upper Saddle River, NJ (1999).
16. Q. Guo, V. A. Sethuraman, and R. E. White, *J. Electrochem. Soc.*, **151**, A983 (2004).
17. J. N. Reimers and J. R. Dahn, *J. Electrochem. Soc.*, **139**, 2091 (1992).
18. Z. Chen, Z. Lu, and J. R. Dahn, *J. Electrochem. Soc.*, **149**, A1604 (2002).
19. M. Broussely, P. Biensan, and B. Simon, *Electrochim. Acta*, **45**, 2 (1999).
20. K. E. Thomas, C. Bogatu, and J. Newman, *J. Electrochem. Soc.*, **148**, A570 (2001).
21. A. T. Stamps, C. E. Holland, R. E. White, and E. P. Gatzke, Private communication.